American Journal of Systems and Software, 2016, Vol. 4, No. 2, 40-45
Available online at http://pubs.sciepub.com/ajss/4/2/2

DOI:10.12691/ajss-4-2-2

Transport of Atmospheric Pollutants in West Mediterranean Areas: Mathematical Model

Josué-Antonio Nescolarde-Selva[1,2,*], José-Luis Usó-Doménech[1], Meng Fan[2]

[1]Department of Applied Mathematics, University of Alicante, Alicante, Spain
[2]School of Mathematics and Statistics, Northeast Normal University, Changchun, China
*Corresponding author: josue.selva@ua.es

Abstract The main objective of this paper is to present a mass conservative method for solving the one-dimensional equation of atmospheric pollutants transport, based on a finite volume method. In order to avoid numerical diffusion a trapezoid rule with a linear interpolation in the extremes of cells is used to approximate integrals. Air pollution problems can be treated by several techniques, we have used a spatial and time uniform grid, numerical results has been implemented in the computer program ATPOTRANS (Atmospheric Pollutants Transport).

Keywords: *atmospheric pollutants, eulerian model, finite volume schemes, grid nodes, numerical schemes*

Cite This Article: Josué-Antonio Nescolarde-Selva, José-Luis Usó-Doménech, and Meng Fan, "Transport of Atmospheric Pollutants in West Mediterranean Areas: Mathematical Model." *American Journal of Systems and Software*, vol. 4, no. 2 (2016): 40-45. doi: 10.12691/ajss-4-2-2.

1. Introduction

Known as the cradle of civilization, the Mediterranean region has been subject to human intervention for millennia, so that little remains of indigenous ecosystems. Yet the region is still an important biological resource. What exactly is the "Mediterranean region"? For the UNEP (United Nations Environment Programme), the Mediterranean region is determined by nature's borders of the "olive tree line". The Mediterranean Sea region — the largest of the semi-enclosed European seas — is surrounded by 22 countries, which together share a coastline of 46 000 km. It is also home to around 480 million people living across three continents: Africa, Asia and Europe. It is still one of the world's busiest shipping routes with about one-third of the world's total merchant shipping crossing the sea each year. Approximately one-third of the Mediterranean population is concentrated along its coastal regions. Meanwhile, about 250 million people (or 55% of the total population) reside in coastal hydrological basins. In the southern region of the Mediterranean [1] 65% of the population (around 120 million inhabitants) is concentrated in coastal hydrological basins, where environmental pressures have increased.

The Mediterranean Sea region has been identified as one of the main climate change hotspots (i.e. one of the areas most responsive to climate change) due to water scarcity, concentration of economic activities in coastal areas, and reliance on climate-sensitive agriculture. However, the region itself emits low levels of greenhouse gases (GHGs) as compared to other areas in the world. Carbon dioxide (CO_2) emissions data show that in 2009, the Mediterranean countries together emitted 6.7% of the world's emissions, equivalent to more than 2 billion tons of CO_2. However, this amount has increased by a factor of 4 in the last 50 years, with an increase in the contribution from countries from the southern region of the Mediterranean from 9% to 30%. Meanwhile, the contribution from all European Union (EU) Mediterranean countries has decreased over the same period from 88% to 54% [4].

The Mediterranean region is characterized by a unique, rich, yet fragile biodiversity, hosted by many diverse ecosystems across the region, which together form an invaluable natural capital on which populations and economies depend. It is estimated that between 10 000 and 12 000 marine species thrive in the Mediterranean Sea. Around 20–30% of these species are endemic. Many of these species are threatened by a range of human activities. Pollution from land-based sources, such as discharges of excess nutrients and hazardous substances, marine litter, over-fishing, and degradation of critical habitats, are responsible for this biodiversity loss. The introduction of invasive alien species presents a threat to the biodiversity, structure, functioning, and stability of the invaded ecosystem. The number of invasive alien species has increased significantly since 1970, and currently stands at around 1 000. Industrial emissions have a heavy impact on the Mediterranean. While pollution from heavy metals in seawater has decreased in recent years, local marine pollution from cities, industry and tourist resorts is still leading to widespread pollution of seas and beaches.

From the perspective of atmospheric pollution, a large number of air quality problems in the southern Europe can

[1] South region is composed of Algeria, Egypt, Israel, Jordan, Lebanon, Libya, Morocco, Syria and Tunisia. All of which, apart from Syria are partners countries under the European Neighbourhood Policy Instrument Shared Environment Information System (ENPI-SEIS) project implemented by the European Environment Agency (EEA) in the period 2010–2015.

be attributed to the existence of recirculatory flows of stagnation episodes with time and space scales of one to several days and tens of kilometers, which are conditioned by the local meteorology and topographical settings [10]. Mediterranean climate was described in the classic text of Barry and Chorley [1]. However, very local, day to day, or hour to hour processes are not duly considered.

Air quality is an important ecological factor for forests, native ecosystems and agricultural crops. Atmospheric pollutants may cause biochemical and physiological damages which lead to reduction of growth and yield [11]. An impairment of competitive and reproductive performance may also occur, which causes changes in species diversity and composition at ecosystem level [13].

The analysis of the historical records of O_3 has revealed a more than two fold increase over the last century [12]. On the basis of present estimates, the global tropospheric concentrations of ozone will continue to increase at a rate faster than during the past 100 years, as a consequence of the continuous increase of the emissions of precursors [6]. Other air pollutants have, at least in some Mediterranean countries, a different trend. This is the case for sulphur dioxide *(*SO_2*)*, whose emissions have been decreasing over the last decade in Italy, France and Spain [2].

Several models are available to calculate short-term concentrations at ground level near a tall stack. In practice, Gaussian models are used in which the values of the dispersion parameters σ_y and σ_z must be given, σ_z, being the most important determining ground level concentration, σ_y and σ_z depend on the stability of the atmosphere. The stability class is usually estimated by using synoptic data such wind speed and cloud cover (for example the Pasquill-Gifford-Turner method). Advantages are the great availability of the input data and the wide applicability of these methods. A great disadvantage is the inaccuracy for the short-term applications. On-line measurement of cloud cover is also a difficulty [3].

The aim of this paper is the numerical simulations of atmospheric pollution transport [5,8]. A model considering this process is based upon a parabolic differential partial equation depending on wind speed, turbulence and diffusion. In addition we need to know the emission rate of the studied pollutants. In order to solve such equation, several numerical schemes based on the finite volume and different standard numerical integration, are presented in this paper. Its accuracy is analyzed in terms of avoid numerical dispersion and spurious oscillations in the resolution of a test problem.

2. Mathematical Model

Air pollution problems can be treated by several techniques, which are mainly divided in two categories: Eulerian models and Lagrangian models. The basic difference between both is that the Eulerian reference system is fixed while the Lagrangian reference system follows the average atmospheric motion. Our model is an Eulerian model.

Let S be a source-sink term due to change of state, chemical transformations, precipitation and sedimentation, $\vec{v}(x,y,z,t)$ be the wind vector, D be the molecular diffusivity (about $1.5\cdot 10^{-5}\, m^2/s$), $\tilde{K}$ be a turbulent diffusivity tensor (3×3) whose elements can be estimated from the output of the meteorological model (e.g. $\vec{v}$, the temperature,…) and $\vec{\nabla}^2 = \frac{\partial^2}{\partial x^2}+\frac{\partial^2}{\partial y^2}+\frac{\partial^2}{\partial z^2}$ be the Laplacian operator, and where we use the so-called K-theory or gradient-transport theory to approximate the turbulent transport. The general mass conservative equation of a single pollutant species of concentration c(x, y, z, t) is:

$$\frac{\partial c}{\partial t} = -\vec{\nabla}(\vec{v}\cdot c)+\vec{\nabla}\cdot\left(\tilde{K}\cdot\vec{\nabla}\cdot c\right)+D\cdot\vec{\nabla}^2\cdot c+S. \qquad (1)$$

In order to solve equation (1), boundary and initial conditions are required. Thus numerical methods allow the computation of approximate solutions using different integration techniques such as:

1) Finite difference methods.
2) Finite element methods.
3) Particle methods.
4) Finite volume methods.

Numerical schemes derived in the paper are based on the finite volume methods. It has several advantages such as the obtaining of a more accurate numerical solution than with finite difference methods and the use of a smaller computation time than finite element methods. The basic difference between the different finite volume schemes is found in the used numerical integration rules. In order to show the advantages and disadvantages of several integration techniques we are going to present several numerical schemes based on finite volume method for solving the above equation (1) and will discuss the purely numerical aspects for getting an accurate numerical scheme. Thus, for the sake of brevity we are going to solve the on-dimensional case:

$$\frac{\partial c}{\partial t}+\frac{\partial}{\partial x}\left(v(x,t)\cdot c\right)-\frac{\partial}{\partial x}\left(k(x,t)\frac{\partial c}{\partial x}\right)=S, \quad \forall x\in\left]0,M\right[,\forall t\in\left]0,T\right[\qquad (2)$$

where we have denoted $k(x,t)=K(x,t)+D$. Moreover a Dirichlet boundary condition is assumed at x = 0 that specify prescribed concentrations in such boundary:

$$c(0,t)=d_0(t) \quad \forall t\in[0,T]$$

with $d_0(t)$ known. Total reflection conditions are assumed at x = L so:

$$k(L,t)\frac{\partial c(L,t)}{\partial x}=0 \quad \forall t\in[0,T].$$

Initial conditions are also required by the time dependent equation (2) and are specified by:

$$c(x,0)=h^0(x) \quad \forall x\in\left]0,M\right[$$

being $h^0(x)$ a known function.

In order to discretize the spatial and temporal domain we divide the intervals $]0,M[$ and $]0,T[$ into cells or control volumes that we denote by E_i, $i=0,...,NX$ for space and T_n, $n=0,...,NT-1$ for time:

$$E_0 = \left[0, x_{\frac{1}{2}}\right], \quad E_i = \left[x_{i-\frac{1}{2}}, x_{i+\frac{1}{2}}\right], \quad i = 1,..., NX-1$$

$$E_{NX} = \left[x_{NX-\frac{1}{2}}, M\right], \quad T_n = \left[t^n, t^{n+1}\right], \quad n = 0,..., NT-1$$

We assume that $x_{i+\frac{1}{2}} - x_{i-\frac{1}{2}} = H_i \quad \forall i = 0,..., NX$ being $x_{-\frac{1}{2}} = 0, x_{NX+\frac{1}{2}}$ and $t^{n+1} - t^n = \Delta t_n$, and also consider:

$$x_0 = 0 \quad x_i = \frac{x_{i+\frac{1}{2}} + x_{i-\frac{1}{2}}}{2}; \quad i = 1,..., NX, \quad x_{NX} = M$$

that we called *grid nodes* and are the values at which we are going to obtain the numerical solutions.

Finite volume method is based on talking a pollutants mass balance over each cell of the temporal and spatial grid:

$$\int_{T_n}\int_{E_i} \frac{\partial c(x,t)}{\partial t} d\Omega + \int_{T_n}\int_{E_i} \frac{\partial \left(v(x,t)\cdot c\right)}{\partial x} d\Omega$$
$$-\int_{T_n}\int_{E_i} \frac{\partial}{\partial x}\left(k(x,t)\frac{\partial c}{\partial x}\right) d\Omega = \int_{T_n}\int_{E_i} S d\Omega$$
$$i = 0,..., NX, \quad n = 0,..., NT-1, \quad \Omega =]0, M[\times]0, T[.$$

The integration over E_0 vanishes because of the Dirichlet condition so their respective equations have been replaced by the equalities:

$$c_0^{n+1} \approx c\left(0, t^{n+1}\right) = d_0\left(t^{n+1}\right), \quad \forall n = 0,..., NT-1.$$

If we use the Green's formula to transform the second and third integrals on the left hand side to integrals over the boundary of cell, we obtain:

$$\int_{E_i} c\left(x, t^{n+1}\right) dx + \int_{T_n} \begin{pmatrix} v\left(x_{i+\frac{1}{2}}, t\right) c\left(x_{i+\frac{1}{2}}, t\right) \\ -v\left(x_{i-\frac{1}{2}}, t\right) c\left(x_{i-\frac{1}{2}}, t\right) \end{pmatrix} dt$$
$$-\int_{T_n} \begin{pmatrix} k\left(x_{i+\frac{1}{2}}, t\right) \dfrac{\partial c\left(x_{i+\frac{1}{2}}, t\right)}{\partial x} \\ +k\left(x_{i-\frac{1}{2}}, t\right) \dfrac{\partial c\left(x_{i-\frac{1}{2}}, t\right)}{\partial x} \end{pmatrix} dt \qquad (3)$$
$$= \int_{E_i} c\left(x, t^n\right) dx + \int_{T_n}\int_{E_i} S d\Omega,$$
$$i = 1,..., NX, \quad n = 0,..., NT-1$$

Typically finite volume methods lump the storage integrals. Thus we use the following approximations:

$$\int_{E_i} g(x) dx \approx H_i g(x_i);$$
$$\int_{T_n} h(t) dt \approx \Delta t_n h\left(t^n\right) \qquad (4)$$

In this way we obtain the next:

$$H_i\left(c_i^{n+1} - c_i^n\right) dx + \Delta t_n \begin{pmatrix} v\left(x_{i+\frac{1}{2}}, t^n\right) c^n\left(x_{i+\frac{1}{2}}\right) \\ -v\left(x_{i-\frac{1}{2}}, t^n\right) c^n\left(x_{i-\frac{1}{2}}\right) \end{pmatrix}$$
$$-\Delta t_n \begin{pmatrix} k\left(x_{i+\frac{1}{2}}, t^n\right) \dfrac{\partial c^n\left(x_{i+\frac{1}{2}}\right)}{\partial x} \\ +k\left(x_{i-\frac{1}{2}}, t^n\right) \dfrac{\partial c^n\left(x_{i-\frac{1}{2}}\right)}{\partial x} \end{pmatrix}$$
$$= \int_{T_n}\int_{E_i} S d\Omega$$
$$i = 1,..., NX, \quad n = 0,..., NT-1$$

being $c^n \approx c\left(x_i, t^n\right)$.

We have to interpolate the solution and to approach its spatial concentration derivative in the extremes of cells as function of its value in the grid nodes.

We assume there exists a uniform gradient between two grid nodes so we approach:

$$k\left(x_{i+\frac{1}{2}}, t^n\right) \frac{\partial c^n\left(x_{i+\frac{1}{2}}\right)}{\partial x} \approx k\left(x_{i+\frac{1}{2}}, t^n\right) \frac{c_{i+1}^n - c_i^n}{h_{i+1}} \qquad (5)$$

being $h_{i+1} = x_{i+1} - x_i$. Notice that because of the Neuman boundary condition at $x = L$.

$$k(L,t) \frac{\partial c(L,t)}{\partial x} = 0 \quad \forall t \in [0,T].$$

If we use the following approximation:

$$v\left(x_{i+\frac{1}{2}}, t^n\right) c^n\left(x_{i+\frac{1}{2}}, t^n\right) - v\left(x_{i-\frac{1}{2}}, t^n\right) c^n\left(x_{i-\frac{1}{2}}\right) \qquad (6)$$
$$\approx v\left(x_i, t^n\right)\left(c_i^n - c_{i-1}^n\right) \quad if \quad v\left(x_i, t^n\right) \geq 0$$

$$v\left(x_{i+\frac{1}{2}}, t^n\right) c^n\left(x_{i+\frac{1}{2}}, t^n\right) - v\left(x_{i-\frac{1}{2}}, t^n\right) c^n\left(x_{i-\frac{1}{2}}\right) \qquad (7)$$
$$\approx v\left(x_i, t^n\right)\left(c_{i+1}^n - c_i^n\right) \quad if \quad v\left(x_i, t^n\right) < 0.$$

The obtained numerical scheme is the same that the obtained with an upstream finite difference approximation forward in time. Such a scheme shows numerical diffusion

that increase when $\frac{v.\Delta t_n}{h_i}$ is smaller. In order to avoid this problem we have designed the following approximation based on a linear interpolation:

$$v^n\left(x_{i+\frac{1}{2}}\right)c^n\left(x_{i+\frac{1}{2}}\right)\approx v\left(x_{i+\frac{1}{2}}\right)\left(\begin{array}{l}\frac{H_{i+1}}{2\cdot h_{i+1}}c_i^n\\ +\frac{H_i}{2\cdot h_{i+1}}c_{i+1}^n\end{array}\right),$$

$$i=1,...,NX-2$$

$$v^n\left(x_{\frac{1}{2}}\right)c^n\left(x_{\frac{1}{2}}\right)\approx v^n\left(x_{\frac{1}{2}}\right)\left(\frac{H_1}{2\cdot h_1}c_0^n+\frac{H_0}{h_1}c_1^n\right) \quad (8)$$

$$v^n\left(x_{NX-\frac{1}{2}}\right)c^n\left(\left(x_{NX-\frac{1}{2}}\right)\right)$$

$$\approx v^n\left(x_{NX-\frac{1}{2}}\right)\left(\frac{H_{NX}}{h_{NX}}c_{NX-1}^n+\frac{H_{NX-1}}{2\cdot h_{NX}}c_{NX}^n\right).$$

Were we have denoted $v^n\left(x_{i+\frac{1}{2}}\right)\approx v\left(x_{i+\frac{1}{2}},t^n\right)$.

However this scheme does not preserve the maximum principle property (Ikeda, 1983), and its solutions may oscillate strongly with respect to both the time and spatial variables when $\frac{v.H}{h}$ is not sufficiently small.

In order to avoid these problems, we replace the above integrals approximation (4) and we assume a linear variation of the pollutants concentration. Thus the numerical integration is the following:

$$\int_{x_{i-\frac{1}{2}}}^{x_{i+\frac{1}{2}}}c^n(x)dx\approx\left(c_{i-1}^n+\frac{H_{i-1}}{2\cdot h_i}\left(c_i^n-c_{i-1}^n\right)\right)\frac{H_i}{2}$$

$$+\left(c_i^n+\frac{H_i}{2\cdot h_{i+1}}\left(c_{+1i}^n-c_i^n\right)\right)$$

$$\frac{H_i}{2}=\left[\begin{array}{l}\left(1-\frac{H_{i-1}}{2\cdot h_i}\right)c_{i-1}^n+\left(\frac{H_{i-1}}{2\cdot h_i}+\left(1-\frac{H_i}{2\cdot h_{i+1}}\right)\right)c_i^n\\ +\frac{H_i}{2\cdot h_{i+1}}c_{i+1}^n\end{array}\right]\frac{H_i}{2}$$

$$i=2,...,NX-1$$

$$\int_{x_{\frac{1}{2}}}^{x_{\frac{3}{2}}}c^n(x)dx\approx\left[\begin{array}{l}\left(1-\frac{H_0}{h_1}\right)c_0^n+\left(\frac{H_0}{h_1}+\left(1-\frac{H_1}{2\cdot h_2}\right)\right)c_1^n\\ +\frac{H_1}{2\cdot h_2}c_2^n\end{array}\right]\frac{H_1}{2}$$

$$\int_{x_{NX-\frac{1}{2}}}^{x_{NX+\frac{1}{2}}}c^n(x)dx\approx\frac{H_{NX}}{2}\left[\begin{array}{l}\frac{H_{NX-1}+H_{NX}}{h_{NX}}c_{NX}^n\\ +\frac{H_{NX}}{h_{NX}}u_{NX-1}^n\end{array}\right]$$

However, the numerical scheme obtained with this approximation (5) and (8) is not stable.

We have also to change the approximation for time integrals. In this case we have to use the following:

$$\int_{T_n}h(t)dt\approx\Delta t_n\left((1-\theta)h\left(t^n\right)+\theta h\left(t^{n+1}\right)\right),\quad\theta\in\left[\frac{1}{2},1\right] \quad (9)$$

For the sake of stability, being h a generical function.

3. Numerical Results

Numerical results has been implemented in the computer program ATPOTRANS (Atmospheric Pollutants Transport). In this case we use θ = 0.5 because a higher θ-value introduces numerical diffusion. With this time integration, numerical scheme is stable for all spatial and time discretizations.

In this paper we tested ATPOTRANS with the following data:

$$v = 5\ km/s$$

$$k = 0.2\ km^2/s$$

assuming a uniform toxic leak with $d_0(t) = 1\ kg/m^2$ and initial concentration being equal to zero $h^0(x) = 0$, $\forall x\in\left]0,M\right[$.

We have used a spatial and time uniform grid with

$$H_i = H,\ \forall i=1,...,NX-1$$

$$H_0 = H_{NX} = \frac{H}{2}$$

$$\Delta t_n = \Delta t,\ \forall n=0,...,NT-1.$$

In this case for avoiding oscillations we have to choose Δt and H so $\frac{v.\Delta t}{h}\le 1$.

Plots obtained are showed in Figure 1 and Figure 2.

4. Conclusions

A better knowledge of air quality is essential, and a greater number of monitoring stations at rural and natural sites is required. The use of biological indicators may provide extremely useful data because of the high density of measuring points which can be covered with relatively little expense [9]. As far as experimental research is concerned, controlled fumigation systems should be set up for operating under field or near-field conditions: open-air fumigation systems and open-top field chambers seem to be the best choice.

An important application for this scheme is to predict emission levels produced for a toxic leak at a determinate distance from the source. For example, this scheme is useful for predicting emission levels of chlorine or another toxic gas, in a leak from a chemical plant in a site at a given distance. Fire brigades can measure wind direction and speed and the flow of pollutant and decide with these data if it is necessary lift out people who lives in a determinate site of a city near the chemical plant.

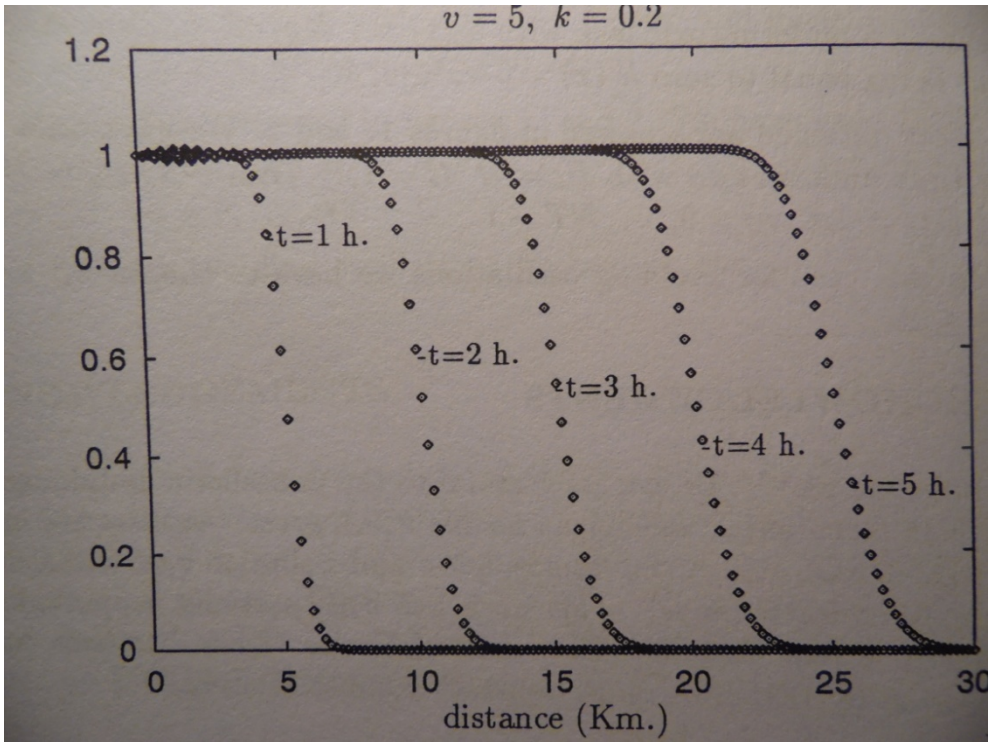

Figure 1. According to the distance

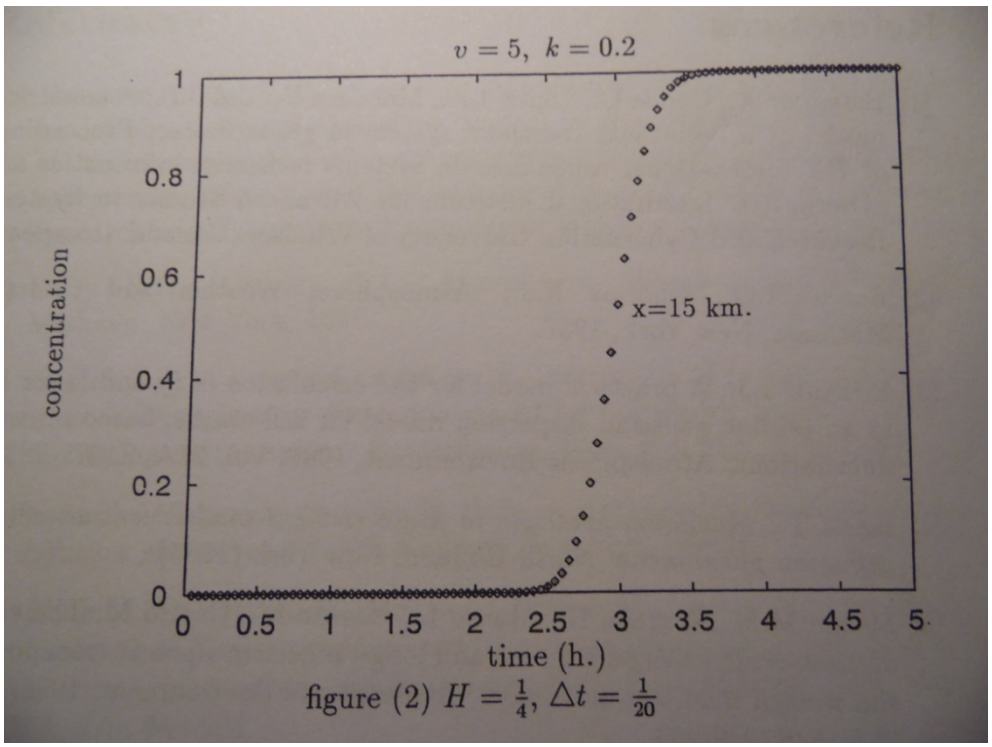

Figure 2. Concentration and time

References

[1] Barry, R.G. and Chorley, R.J. 1987. *Atmosphere, Weather and Climate*. Methuen. New York.

[2] EMEP. 1990. *Calculated budgets of airborne sulphur and nitrogen over Europe*. EMEP Report MSC-W *2/90.*

[3] Erbrink, J.J. 1991. A practical model for the calculation of σ_y and σ_z for use in an on-line Gaussian dispersion model for tall stacks, based on wind fluctuations. *Atmospheric Environment*. Vol 25A, 2, pp 277-283.

[4] Giorgi, F., 2006, Climate change hot-spots. *Geophysical Research Letters* 33(8), pp. L08707.

[5] Hagler, G. S. W., Tang, W. 2016. Simulation of rail yard emissions transport to the near-source environment. *Atmospheric Pollution Research.* 7(3). pp. 469-476.

[6] Hough A.M, Derwent R.G. 1990. Changes in the global concentration of tropospheric ozone due to human activities. *Nature*, 344, pp 645-648.

[7] Ikeda, T. 1983. *Maximum principle in finite element models for convection diffusion phenomena*. North Holland. New York.

[8] Liu, Z., Wang, L., Zhu, H. 2015. A time–scaling property of air pollution indices: a case study of Shanghai, China. *Atmospheric Pollution Research*. 6(5). pp. 886-892.

[9] Mignanego L., Biondi F., Schenone G. 1992. Ozone biomonitoring in northern Italy. *Agriculture, Ecosystems and Environment*, 21 , pp 141-159.

[10] Millan, M.M., Artiano, B., Alonso, L., Navazo, M. and Castro, M. 1991. The effect of meso-scale flows on regional and long-range atmospheric transport in the western Mediterranean area. *Atmospheric Environment*. Vol 25A, 5/6, pp 949-963.

[11] Treshow M. (ed.). 1984. *Air pollution and plant life.* John Wiley & Sons, Chichester, New York.

[12] Volz A., Kley D. 1988. Evaluation of the Montsouris series of ozone measurements made in the nineteenth century. *Nature*, 332, pp 240-242.

[13] Westman W.E. 1985. Air pollution injury to coastal sage scrub in the Santa Monica Mountains, Southern California. *Water, Air, and Soil Pollution*, 26, pp 19-41.